ORIGINAL ARTICLE

Evaluation of Tissue Behavior on Three-dimensional Collagen Scaffold Coated with Carbon Nanotubes and β-tricalcium Phosphate Nanoparticles

Hirofumi MIYAJI[1], Shusuke MURAKAMI[1], Erika NISHIDA[1], Tsukasa AKASAKA[2], Bunshi FUGETSU[3], Junko UMEDA[4], Katsuyoshi KONDOH[4], Tadashi IIZUKA[5], and Tsutomu SUGAYA[1]

[1] Department of Periodontology and Endodontology,
[2] Department of Biomedical Materials and Engineering,
Faculty of Dental Medicine, Hokkaido University, Sapporo, Japan
[3] Policy Alternatives Research Institute, The University of Tokyo, Tokyo, Japan
[4] Joining and Welding Research Institute, Osaka University, Osaka, Japan
[5] Support Section for Education and Research, Faculty of Dental Medicine, Hokkaido University, Sapporo, Japan

SYNOPSIS
We generated a three-dimensional collagen scaffold coated with carbon nanotubes (CNTs) and β-tricalcium phosphate (β-TCP) nanoparticles and histologically evaluated tissue behavior toward the nanomodified scaffold after subcutaneous tissue implantation in rat. Scanning electron microscopy images of the nanomodified scaffold showed that the collagen surface was enveloped by a meshwork of CNTs and dispersed β-TCP nanoparticles. Histological observations indicated that application of CNTs and β-TCP nanoparticles increased cell and blood vessel penetration into the collagen scaffold. CNTs consistently stimulated giant cell aggregation. In addition, CNTs and β-TCP application to the scaffold significantly promoted the DNA content of infiltrating cells and scaffold biodegradation compared to the untreated scaffold. The nanomodified scaffold coated with CNTs and β-TCP nanoparticles would be beneficial for tissue engineering therapy.

***Key words**: biocompatibility, nanocarbon, rat, tissue engineering*

INTRODUCTION

A tissue engineering strategy requires three biological elements: cells, molecules and scaffolds[1]. It was reported that the surface nanostructure of a scaffold plays a major role in upregulating cell proliferation and differentiation after implantation into the body[2]. The nanostructured surface obviously increases the surface area and roughness of the scaffold to promote subsequent molecular adsorption and cellular

behavior[3,4]. Thus, nanomodification of the scaffold would be beneficial for predictable tissue regeneration.

Carbon-based nanomaterials have been extensively examined for biomedical applications[5,6]. In particular, carbon nanotubes (CNTs) have novel and unique biological and electrical properties, and are anticipated to be used as biomedical devices for drug delivery and as tissue engineering scaffolds. Akasaka *et al*. reported that CNTs effectively induced the growth of apatite crystallites on their surfaces in a calcium phosphate (CP) solution[7]. In addition, CNT-modified biomaterials enhanced the early attachment and proliferation of MC3T3-E1 cells[8,9]. Hence, application of nanomodified CNTs could provide bone-inducting properties to scaffolds and be beneficial for bone tissue engineering.

Bioceramics, such as CP and hydroxyapatite (HA), are widely known as bio-safe materials and bone graft substitutes[10,11]. Resorption of bioceramics is generally intractable; however, nanosized bioceramics could be resorbed by phagocytosis of macrophages to subsequently release calcium and phosphate ions. Reportedly, scaffolds coated with CP nanoparticles exhibited high osteoinductivity. Ibara *et al*. and Murakami *et al*. reported that a collagen scaffold coated with β-tricalcium phosphate (β-TCP) nanoparticles promoted the proliferation of attached cells and bone augmentation of rat skull[12,13]. Ogawa *et al*. demonstrated remarkable periodontal alveolar bone healing with an implanted nano-β-TCP scaffold[14]. In addition, Joseph *et al*. generated a collagen scaffold coated with nanostructured HA which was subsequently implanted into rat dorsal subcutaneous tissue. They showed that cell and blood vessel penetration into the scaffold was significantly facilitated[15].

Accordingly, we speculated that nanomodification of a collagen scaffold via application of CNTs and CP nanoparticles could promote its bioactivities. In this study, we produced a collagen scaffold coated with CNTs and β-TCP nanoparticles and assessed tissue behavior in comparison to an untreated scaffold.

MATERIALS AND METHODS

Generation and characterization of scaffolds

Multi-walled CNTs (Nanocyl NC7000, 9.5 nm diameter; Nanocyl, Sambreville, Belgium) were used in this study. β-TCP powder (Beta TCP; Tomita Pharmaceutical Co. Ltd., Naruto, Japan) was pulverized into nanosized particles using a pulverizer (Nanomizer Inc., Yokohama, Japan). CNTs and β-TCP nanoparticles were then dispersed in 1-methyl-2-pyrrolidone (Wako Pure Chemical Industries Ltd., Osaka, Japan) along with the surfactant sodium cholate (0.2 wt%). Dispersion doses of CNTs and β-TCP nanoparticles were 0.1 and 1 wt%, respectively.

Dispersions of CNTs and/or β-TCP nanoparticles were injected into a collagen scaffold (Terudermis®; 6 × 6 × 3 mm; Olympus Terumo Biomaterials Corp., Tokyo, Japan) using a syringe with a 25-gauge needle. Next, the scaffold was thoroughly washed in ethanol to remove the dispersion solution. After air-drying, scaffolds were obtained for assessment and labeled respectively as CNT, TCP and CNT/TCP scaffolds (Figure 1A, B and C). Untreated collagen scaffold was assessed as a negative control (Figure 1D).

The scaffold blocks were cut through the center and characterized using a scanning electron microscope (SEM, S-4000; Hitachi Ltd., Tokyo, Japan) with an accelerating voltage of 10 kV after coating with a thin layer of Pt-Pd.

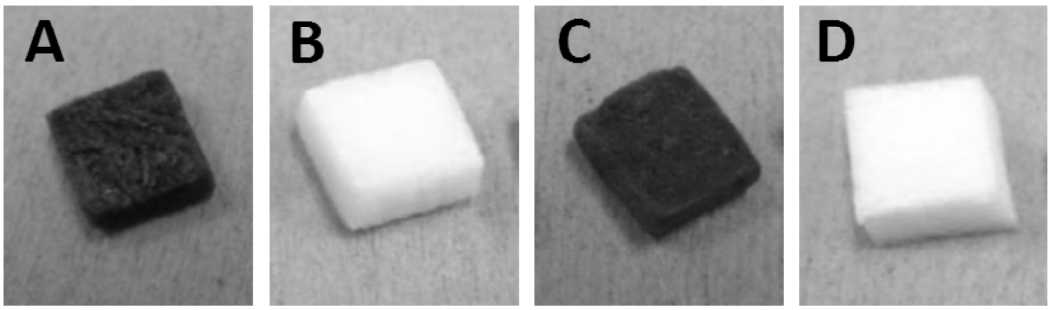

Figure 1 Digital images of CNT (A), TCP (B), CNT/TCP (C) and untreated (D) scaffolds.

Assessment of rat subcutaneous tissue behavior

Animal experimental protocols followed the institutional animal use and care regulations of Hokkaido University (Animal Research Committee of Hokkaido University, approval number 10–42). Ten-week-old male Wistar rats weighing 190–210 g each were given general anesthesia by intraperitoneal injection of 0.6 mL/kg sodium pentobarbital (Somnopentyl; Kyoritsu Seiyaku Corp., Tokyo, Japan) as well as a local injection of 2% lidocaine hydrochloride with 1:80,000 epinephrine (Xylocaine Cartridge for Dental Use; Dentsply Sankin K.K., Tokyo, Japan). After a dorsal skin incision was made in each rat, the scaffold was implanted into the subcutaneous tissue. Skin flaps were sutured (Softretch 4-0; GC, Tokyo, Japan) and tetracycline hydrochloride ointment (Achromycin Ointment; POLA Pharma Inc., Tokyo, Japan) was applied to the wound. Rats were euthanized by administration of an overdose of sodium pentobarbital (2.0 mL/kg) at 10 days post-surgery.

For DNA measurement (n=7), the implanted scaffolds were extracted from the wounds and freeze-dried. After pulverization, 0.5 mL of 2 M NaCl and 0.05 M phosphate buffer (pH 7.4) were added to each scaffold. After centrifugation, the DNA content of the infiltrated cells into the scaffold was measured with a DNA quantification kit (Primary Cell Co. Ltd., Sapporo, Japan) according to the manufacturer's instructions, using a fluorescence spectrophotometer (F-3000; Hitachi Ltd.) equipped with a 356-nm excitation filter and a 458-nm emission filter.

For histologic measurements (n=5), tissue blocks were fixed in 10% buffered formalin, embedded in paraffin wax, and cut into 5-μm sections. Sections were stained with hematoxylin-eosin and observed histologically using light microscopy. Histomorphometric measurements of the residual scaffold were carried out using Image J software (ver. 1.41; National Institutes of Health, Bethesda, MD, USA). In addition, three area units (0.12 mm^2 per unit) at the peripheral area of the scaffold were selected and foreign body giant cells in the unit were counted under a light microscope.

Statistical analysis

The mean and standard deviation of each parameter were calculated for each group. Differences between groups were analyzed using the Scheffé test. Results were regarded as statistically significant at $P < 0.05$. All statistical analyses were performed using SPSS software (SPSS 11.0; IBM Corporation, Armonk, NY, USA).

RESULTS

Characterization of scaffolds

SEM images of the inner region of nanomodified scaffolds are shown in Figure 2. The CNT scaffold showed that the meshwork of CNTs, CNT-net, was uniformly generated on the collagen strut surface (Figure 2A). In the TCP scaffold, we confirmed that the β-TCP nanoparticles were attached well to the collagen and the size of β-TCP nanoparticles was approximately 100–500 nm (Figure 2B). In the CNT/TCP scaffold, the surface of the β-TCP nanoparticles and the collagen surface were frequently enveloped by the CNT-net (Figure 2C). Large aggregates of CNTs and β-TCP were rarely observed. The interconnected structure of the collagen scaffold appeared after coating with CNTs and β-TCP nanoparticles (Figure 2D). In the control, no structures besides the collagen strut were observed (Figure 2E).

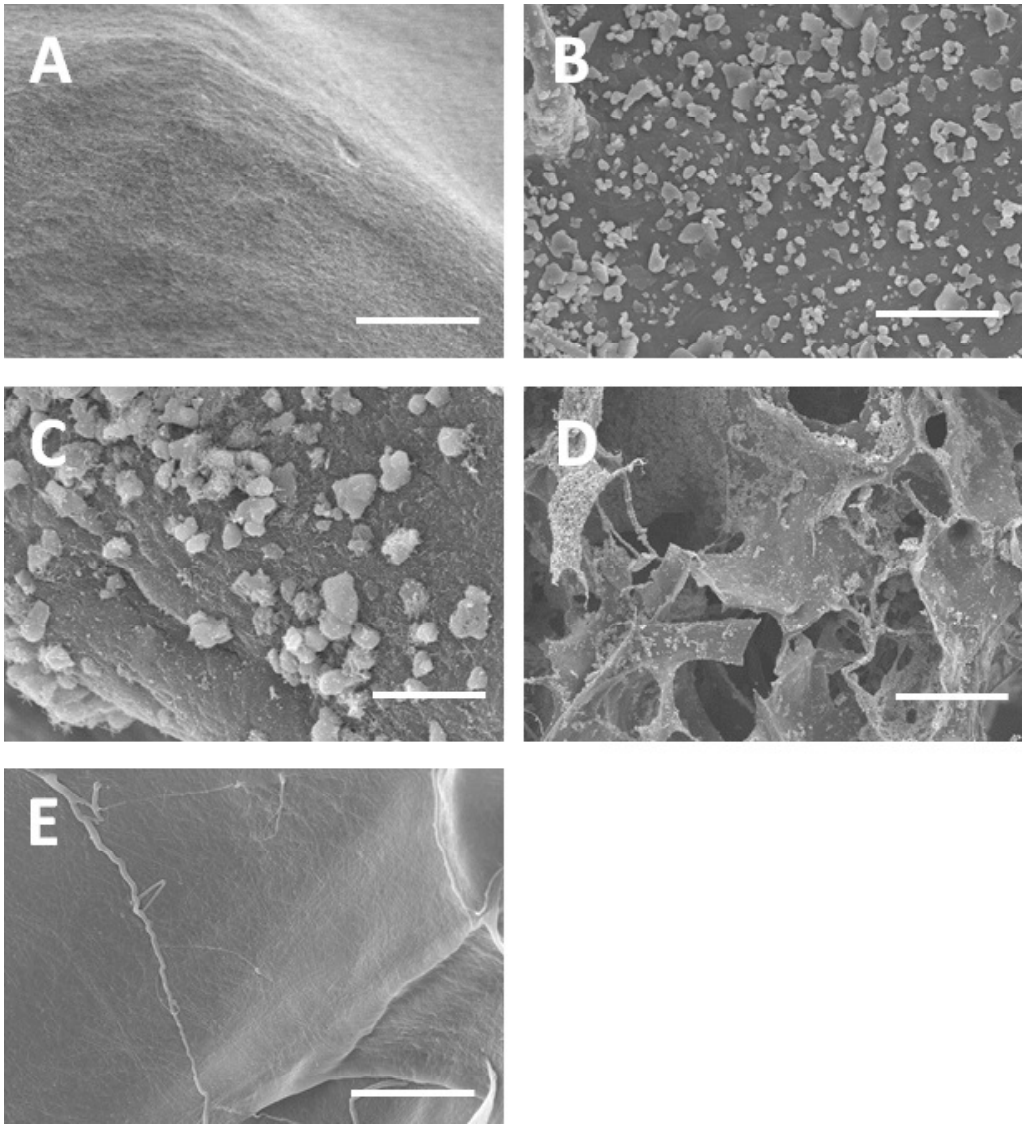

Figure 2 SEM micrographs of CNT (A), TCP (B), CNT/TCP (C and D) and untreated (E) scaffolds. Scale bars are 10 μm (A, B and E), 3 μm (C) and 150 μm (D).

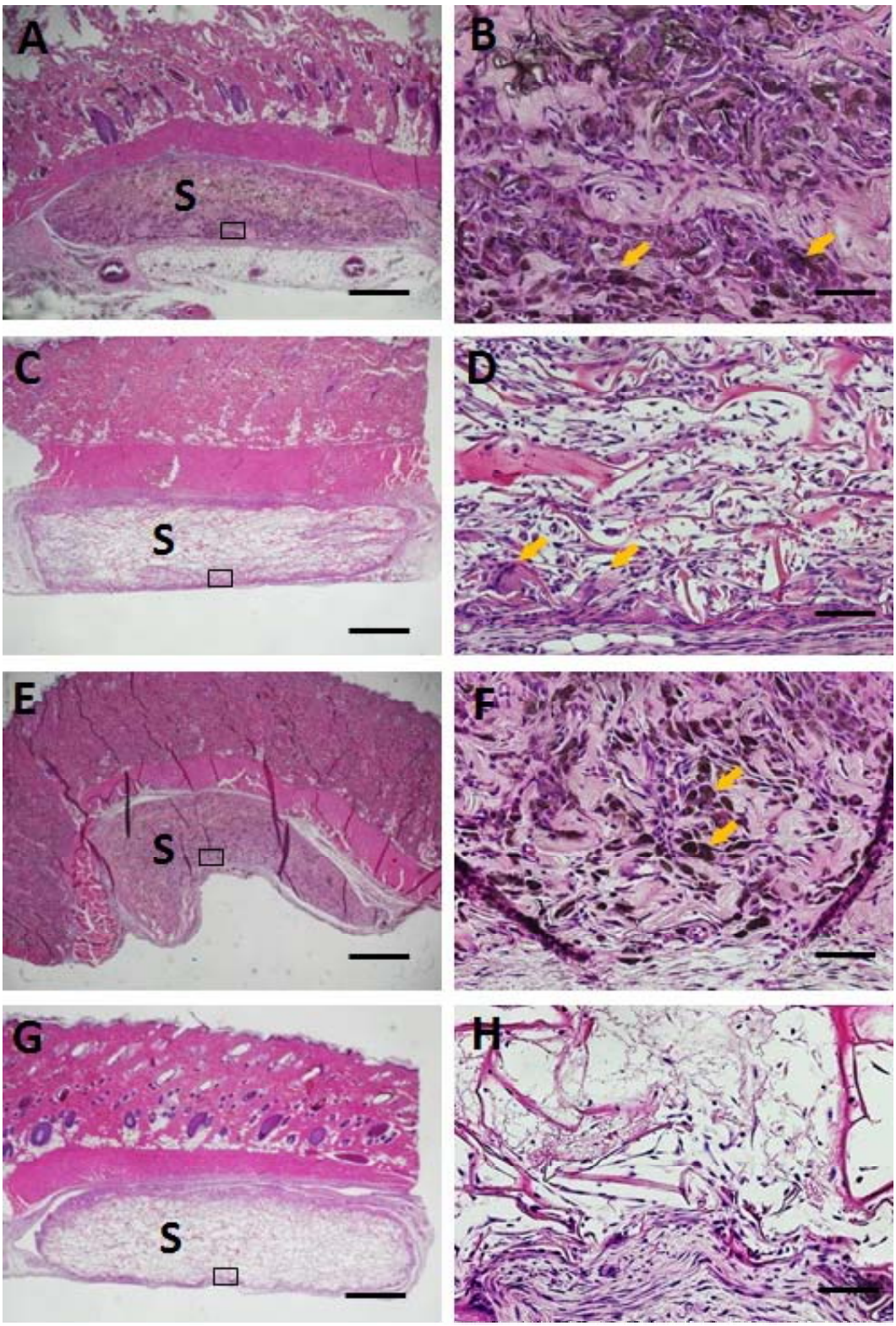

Figure 3 Histologic findings in rat subcutaneous tissue at 10 days for implanted CNT (A and B), TCP (C and D), CNT/TCP (E and F) and untreated (G and H) scaffolds. (B), (D), (F) and (H) represent higher magnifications of the framed areas in (A), (C), (E) and (G), respectively. Abbreviations: S denotes scaffold. Scale bars are 1 mm (A, C, E and G) and 100 μm (B, D, F and H). Arrows indicate giant cells. Staining: hematoxylin-eosin.

Assessment of tissue behavior in rats

The nanomodified scaffold consistently increased cell and blood vessel penetration into the scaffold in comparison to the untreated scaffold. The CNT scaffold consistently contained high-density and blackened giant cells in the center of the scaffold (Figure 3A and B). Rats implanted with the TCP scaffold showed penetration of fibroblastic cells and blood vessels into the scaffold, and foreign body giant cells were located at the peripheral area of the scaffold (Figure 3C and D). Animals implanted with the CNT/TCP scaffold exhibited penetration of blackened giant cells as observed for the CNT scaffold (Figure 3E and F). In the untreated scaffold group, the inner region was occupied by a fibrin network and sparse cells (Figure 3G and H). All specimens showed that inflammatory cell filtration was rarely demonstrated in the subcutaneous tissue around the implanted scaffold.

Nanomodification of the scaffold remarkably increased the DNA content of infiltrating cells compared to the untreated scaffold. No significant difference was found between the CNT, TCP and CNT/TCP scaffold implantations (Figure 4A). The area of residual nanomodified scaffold was decreased in all samples, with CNT and CNT/TCP scaffolds significantly lower than the untreated scaffold (Figure 4B). CNT implantation significantly promoted the aggregation of giant cells in the scaffold. The number of giant cells in the CNT and CNT/TCP scaffolds was approximately 5- and 3-fold greater than the TCP scaffold, respectively (Figure 4C).

DISCUSSION

Nanomodification of the scaffold remarkably promoted the DNA content of penetrating cells. It was suggested that nanomaterial application stimulated cell migration and proliferation. As the nanostructure results in greater surface area, the nanomodified surface enhances the absorption of proteins[16,17]. Hence, CNT, TCP and CNT/TCP scaffolds likely possess bioactive protein molecules, derived from the tissue fluid, which are capable of promoting cellular behaviors following implantation. In this study, the cellular ingrowth area of each scaffold frequently involved the formation of blood vessels. In particular, blood vessel formation would be beneficial for tissue reconstruction via the supply of nutritional factors and oxygen.

Histological images showed the

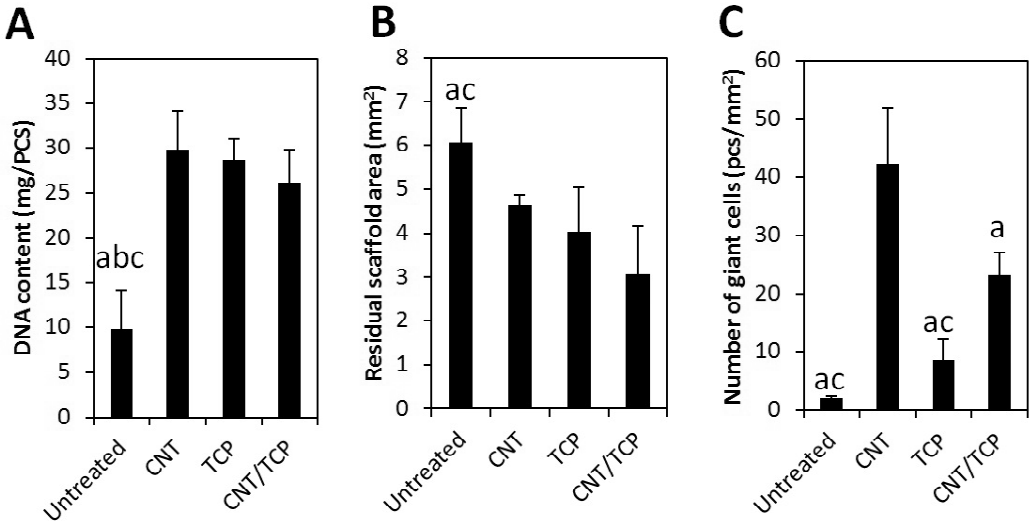

Figure 4 Measurements of DNA content (A), residual scaffold area (B) and number of giant cells at 10 days (A; n=7, mean ± SD and B and C; n=5, mean ± SD). a, $P < 0.05$ vs. CNT; b, $P < 0.05$ vs. TCP; c, $P < 0.05$ vs. CNT/TCP.

presence of numerous giant cells in the CNT scaffold. In addition, examination of giant cell numbers revealed that the CNT modification consistently increased the appearance of giant cells. It was suggested that CNT application stimulated macrophage accumulation against the implanted scaffold and that the subcutaneous tissue behavior differed according to the type of nanomaterial. In general, macrophages accelerate the resorption of implanted biomaterial via phagocytosis. However, residual scaffold measurement revealed that the degradation of the CNT scaffold was comparable to that of the TCP scaffold showing slight giant cell accumulation. We suggest that the macrophages stimulated by CNT application exert various bioactive effects as well as scaffold resorption. Wang *et al*. demonstrated that macrophages exhibited immuno-modulatory effects against bioactive materials and subsequently enhanced angiogenesis and osteogenesis[18]. In addition, Nishida *et al*. reported that the nanocarbon material graphene oxide recruits wound healing macrophages (M2 macrophage) associated with immunosuppression as well as tissue repair and remodeling[5].

Regarding the biocompatibility of each scaffold, inflammatory cell infiltration was rarely observed surrounding the connective tissue. However, the CNT scaffold was observed in the presence of blackened giant cells, suggesting that CNTs are frequently phagocytized by giant cells. Recent studies showed the accumulation of blackened macrophage-like cells on a CNT substrate[9,19]. Sato *et al*. reported that narrow diameter (15 nm) CNTs were gradually degraded within the lysosomes of macrophages and no symptoms of cancer or severe inflammatory reactions were displayed[20]. The long-term degradation of CNT scaffolds should be further evaluated in the future.

CONCLUSION

We generated scaffolds using CNTs and/or β-TCP nanoparticle application and investigated tissue behaviors after implantation into rat subcutaneous tissue. The nanomodified scaffold promoted cell and blood vessel penetration compared to the untreated scaffold. Furthermore, nanomodification with CNTs clearly stimulated giant cell aggregation.

ACKNOWLEDGEMENTS

The authors would like to thank Olympus Terumo Biomaterials for providing collagen scaffolds and Tomita Pharmaceutical for providing β-TCP. This work was supported by the Akiyama Life Science Foundation Grant Program and JPSP KAKENHI Grant Numbers 16K11822, 16H06604 and 25463210. This work was performed under the cooperative research program of the Joining and Welding Research Institute, Osaka University. The authors report no conflict of interest related to this study.

REFERENCES

1) Yoshida T, Miyaji H, Otani K, Inoue K, Nakane K, Nishimura H, Ibara A, Shimada A, Ogawa K, Nishida E, Sugaya T, Sun L, Fugetsu B, Kawanami M. Bone augmentation using a highly porous PLGA/b-TCP scaffold containing fibroblast growth factor-2. J Periodont Res 2015;50:265-273.
2) Zinger O, Anselme K, Denzer A, Habersetzer P, Wieland M, Jeanfils J, Hardouin P, Landolt D. Time-dependent morphology and adhesion of osteoblastic cells on titanium model surfaces featuring scale-resolved topography. Biomaterials 2004; 25: 2695-2711.
3) Woo KM, Chen VJ, Ma PX. Nano-fibrous scaffolding architecture selectively enhances protein adsorption contributing to cell attachment. J Biomed Mater Res A 2003; 67: 531-537.
4) Wei G, Ma PX. Structure and properties of nano-hydroxyapatite/polymer composite scaffolds for bone tissue engineering. Biomaterials 2004; 25: 4749-4757.
5) Nishida E, Miyaji H, Kato A, Takita H, Iwanaga T, Momose T, Ogawa K,

Murakami S, Sugaya T, Kawanami M. Graphene oxide scaffold accelerates cellular proliferative response and alveolar bone healing of tooth extraction socket. Int J Nanomed 2016; 11: 2265-2277.
6) Hirata E, Miyako E, Hanagata N, Ushijima N, Sakaguchi N, Russier J, Yudasaka M, Iijima S, Bianco A, Yokoyama A. Carbon nanohorns allow acceleration of osteoblast differentiation via macrophage activation. Nanoscale 2016; 8: 14514-14522.
7) Akasaka T, Watari F, Sato Y, Tohji K. Apatite formation on carbon nanotubes. Mater Sci Eng C 2006; 26: 675-678.
8) Hirata E, Uo M, Takita H, Akasaka T, Watari F, Yokoyama A. Development of a 3D collagen scaffold coated with multiwalled carbon nanotubes. J Biomed Mater Res B Appl Biomater 2009; 90: 629-634.
9) Nishida E, Miyaji H, Umeda J, Kondoh K, Takita H, Kanayama I, Tanaka S, Kato A, Fugetsu B, Akasaka T, Kawanami M. Biological response to nanostructure of carbon nanotube/titanium composite surfaces. Nano Biomed 2015; 7; 11-20.
10) Zheng H, Bai Y, Shih MS, Hoffmann C, Peters F, Waldner C, Hübner WD. Effect of a β-TCP collagen composite bone substitute on healing of drilled bone voids in the distal femoral condyle of rabbits. J Biomed Mater Res B Appl Biomater 2014; 102: 376-383.
11) Yuan H, van Blitterswijk CA, de Groot K, de Bruijn JD. Cross-species comparison of ectopic bone formation in biphasic calcium phosphate (BCP) and hydroxyapatite (HA) scaffolds. Tissue Eng 2006; 12: 1607-1615.
12) Ibara A, Miyaji H, Fugetsu B, Nishida E, Takita H, Tanaka S, Sugaya T, Kawanami M. Osteoconductivity and biodegradability of collagen scaffold coated with nano-β-TCP and fibroblast growth factor 2. J Nanomater 2013; 2013: 1-11.
13) Murakami S, Miyaji H, Nishida E, Kawamoto K, Miyata S, Takita H, Akasaka T, Fugetsu B, Iwanaga T, Hongo H, Amizuka N, Sugaya T, Kawanami M. Dose effects of beta-tricalcium phosphate nanoparticles on biocompatibility and bone conductive ability of three-dimensional collagen scaffolds. Dent Mater J 2017; 36: 573-583.
14) Ogawa K, Miyaji H, Kato A, Kosen Y, Momose T, Yoshida T, Nishida E, Miyata S, Murakami S, Takita H, Fugetsu B, Sugaya T, Kawanami M. Periodontal tissue engineering by nano beta-TCP scaffold and FGF-2 in 1-wall infrabony defects of dogs. J Periodont Res 2016; 51: 758-767.
15) Nathanael AJ, Oyane A, Nakamura M, Sakamaki I, Nishida E, Kanemoto Y, Miyaji H. In vitro and in vivo analysis of mineralized collagen-based sponges prepared by a plasma- and precursor-assisted biomimetic process. ACS Appl Mater Interfaces. 2017; 9: 22185-22194.
16) Bacakova L, Filova E, Parizek M, Ruml T, Svorcik V. Modulation of cell adhesion, proliferation and differentiation on materials designed for body implants. Biotechnol Adv. 2011;29:739-767.
17) Li X, Liu H, Niu X, Yu B, Fan Y, Feng Q, Cui FZ, Watari F. The use of carbon nanotubes to induce osteogenic differentiation of human adipose-derived MSCs in vitro and ectopic bone formation in vivo. Biomaterials 2012; 33: 4818-4827.
18) Wang M, Yu Y, Dai K, Ma Z, Liu Y, Wang J, Liu C. Improved osteogenesis and angiogenesis of magnesium-doped calcium phosphate cement via macrophage immunomodulation. Biomater Sci 2016; 4: 1574-1583.
19) Hirata E, M´enard-Moyon C, Venturelli E, Takita H, Watari F, Bianco A, Yokoyama A. Carbon nanotubes functionalized with fibroblast growth factor accelerate proliferation of bone marrow-derived stromal cells and bone formation. Nanotechnology. 2013;24:1-8.
20) Sato Y, Yokoyama A, Nodasaka Y, Kohgo T, Motomiya K, Matsumoto H, Nakazawa E, Numata T, Zhang M, Yudasaka M, Hara H, Araki R, Tsukamoto O, Saito H, Kamino T, Watari F, Tohji K. Long-term biopersistence of tangled oxidized carbon nanotubes inside and outside macrophages in rat subcutaneous tissue. Sci Rep 2013; 3: 1-10.

(Received, November 13, 2017/
Accepted, December 26, 2017)

Corresponding author:
Hirofumi Miyaji, DDS, Ph.D
Department of Periodontology and Endodontology,
Faculty of Dental Medicine,
Hokkaido University
N13 W7 Kita-ku Sapporo 060-8586 Japan.
Tel. +81-11-706-4266
Fax +81-11-706-4334
E-mail: miyaji@den.hokudai.ac.jp